CALIFORNIA INSTITUTE OF TECHNOLOGY

Department of Mechanical and Civil Engineering

Comments on Philippe de la Hire's Memoir on Arch Abutment Design (1712)

CALTECH CIVIL ENGINEERING REPORT NO. 2020-01

John F. Hall

Professor of Civil Engineering

FEBRUARY 2020

CONTENTS

1. INTRODUCTION

Philippe de la Hire (1640-1718), a multi-disciplinary French scientist, is generally credited as being the first person to apply the principles of statics to the analysis and design of arches. Prior efforts employed geometric design rules that were based on experience. Thus, de la Hire plays an important role in the transition to scientifically based methods for civil engineering structures. Therefore, it is of historical interest to understand de la Hire's approach and perspective.

Proposition 125 of de la Hire's *Traité de Mécanique* [1] deals with arches comprised of discrete stones that abut each other along joints that are considered smooth (frictionless). Each stone is subjected to three forces: the weight of the stone and the forces from the two neighboring stones that are oriented perpendicular to the respective joints. For an arch of given shape, the stone-by-stone analysis determines the weights of the stones that are required for equilibrium. This is possible because the weight of the key stone is pre-determined. The analysis works for all the stones except the two at the bottom of the arch (one on each side), for which an infinite weight is required to counter the lack of sliding resistance along the smooth horizontal base. De la Hire salvages his analysis by saying that, in reality, sliding would not occur due to the stones being joined by mortar.

Of interest in this report is another work by de la Hire, his 9-page Memoir of 1712, *Sur la construction des voûtes dans les édifices* [2] (*On the construction of vaults in buildings*). [Memoir in this usage means an essay on a learned subject.] The work focuses on arch abutments, about which de la Hire says: "C'est un problème des plus difficiles qu'il y ait dans l'architecture, …" (It is a problem of the most difficult that there is in architecture, …) De la Hire adds: "Ce problème appartient à la mécanique, & c'est par son moyen que nous pouvons le résoudre, …" (This problem belongs to mechanics, and it is by its means that we can solve it, …)

In the Memoir, an abutment is a free-standing rectangular pier, and the object is to find the width of the pier sufficient to prevent overturning caused by the thrust of the arch. Sliding of the pier on its foundation is assumed to be restrained. De la Hire derives a quadratic equation in terms of the width of the abutment for a circular arch, and then he describes a graphical construction to solve the quadratic equation. He does the same for a *plate-bande* (flat arch).

De la Hire's Memoir contains three figures, and these are copied here to the Appendix. Figure A1 shows the geometry of the circular arch together with one of its abutments (the rectangle $BHSI$). ML represents a joint in the arch. De la Hire's graphical construction for finding the abutment width for the circular arch is shown in Figure A2, and that for the plate-bande appears in Figure A3. The geometry of the plate-bande to the left of the centerline is also visible in Figure A3: abutment $BHSL$, flat half arch $NBEF$ and joint ML.

De la Hire's Memoir has been discussed many times, for example, [3-9]. Nevertheless, there appear to be several areas for further inquiry. In this report:

- Comments are made about how de la Hire thought about the problem of determining abutment width, and a different interpretation is made compared to some other authors.
- De la Hire's method of analysis is reviewed, and a conclusion is reached about the generality of the location where the arch splits, again different compared to some others.
- De la Hire's graphical constructions are analyzed, and a possible discrepancy pointed out previously by Benvenuto [5] is identified and corrected.
- De la Hire's problem of determining abutment width is re-solved with friction included in the arch to assess the complexity added to the solution process and the effect on the answer. Also, results using de la Hire's assumed collapse mechanism are compared to the actual collapse mechanism, which depends on the coefficient of friction.

In the report that follows, de la Hire's original notation has been kept as much as possible. Dimensions are expressed in arbitrary length units, which can be uniformly scaled up or down using any desired length scale.

2. HOW DE LA HIRE VIEWED THE CIRCULAR ARCH

The circular arch considered by de la Hire is 2-dimensional and symmetric with no variations perpendicular to the plane. His diagram from Figure A1 is redrawn in Figure 1. The arch is of uniform thickness and subtends an angle of 180º. The inner edge of each abutment is flush with the intrados of the arch, and the abutments are supported against horizontal displacement at their bases. Self-weight only of the arch and abutments is applied, and the unit weight is uniform. Under these conditions, the weight of a piece can be replaced by its area for the purpose of calculating abutment width.

De la Hire states that when the abutments are too weak to support the thrust from an arch, it is generally noticed that the arch splits at locations toward the middle of each side between the tops of the abutments and the key. De la Hire supposes that the central portion of the arch, above the splits, is well connected and remains solid. The same is assumed for the lower part of the arch on each side attached to the corresponding abutment. Thus, there are three pieces, and one of the two containing an abutment is shown in Figure 2a. The joint where splitting occurs is radial and designated ML. Through this joint acts the thrust from the weight of the half arch segment above, this weight designated here by A (its area). De la Hire places this thrust at the intrados (point L) "suivant la direction des corps pesants", i.e., in the tangential direction, which is normal to the joint. Thus, the magnitude of the thrust is $A/\sin(\theta)$, which has a vertical component

equal to A and where θ is the angle the joint ML makes with vertical. As mentioned later in Section 3, de la Hire never actually expresses the thrust in this form.

De la Hire recognizes that each of the lower pieces resists the thrust by its own weight. When an abutment is just wide enough, it is on the verge of rotating about its bottom outside corner. Thus, de la Hire thinks in terms of a bent lever LHT with fulcrum located at point H; see Figure 2b. Moment equilibrium of the lever (known then as the law of the lever) leads to the equation from which the abutment width can be determined as explained in Section 3.

The reason for placing the joint thrust at the intrados is not stated by de la Hire. Neither does de la Hire explain why he orients the thrust normal to the joint; nowhere does he mention friction or the lack of it. In proposition 125 of his *Traité de Mécanique* [1], he is explicit about the arch joints being smooth, and thus he uses normal thrusts. By the time of his Memoir, de la Hire was aware of the basic concept of friction [10], including the friction force being proportional to the normal force. But he again uses normal thrusts in his Memoir. Neglect of friction makes the analysis easier, and the difficulty that de la Hire encountered in proposition 125 with the infinite stone weights does not arise in his determination of abutment width in the Memoir.

Some authors have concluded that de la Hire based his analysis on a collapse mechanism in which the central part of the arch, acting as a wedge, slides down between the two levers on frictionless joints, rotating the abutments out as depicted in Figure 3 [5-8], "constituting a first example of 'limit analysis' of arches [7]." While such a view is consistent with de la Hire's analysis, including the placement of the joint thrust at the intrados, there is no direct evidence in his writing that he was thinking of the problem in terms of any collapse mechanism that involved the entire structure. He never describes such a mechanism, nor does he ever mention a wedge or even sliding. If de la Hire had a sliding system in mind, he likely would have said something about assumptions regarding friction.

Of course, the abutments cannot rotate out without the central portion of de la Hire's three-piece arch sliding down. And it seems obvious that this rotation moves the contact in the arch joint to the intrados. But, again, de la Hire does not indicate completeness of thought in terms of a collapse mechanism for the entire structure. Kurrer [8] describes only one instance of a collapse mechanism being discussed that pre-dates de la Hire's Memoir (attributed to Bernardino Baldi, an Italian mathematician), and he suggests this work may have been unknown to the French scientists. Belidor [11], who followed de la Hire, places the arch thrust at the middle of the joint. So, if de la Hire was thinking in terms of a collapse mechanism, Belidor apparently never realized or accepted it.

Nevertheless, de la Hire succeeds in separating a complex structure into pieces, and then applying the principles of statics to obtain a design parameter, possibly the first ever such application for any type of structure, which is a significant accomplishment.

3. EQUATION FOR ABUTMENT WIDTH FOR THE CIRCULAR ARCH

De la Hire's model involves three pieces: the central portion of the arch above the joints ML and the two parts below these joints, each of which includes a lower part of the arch and one of the abutments. One of these latter parts, shown in Figure 2, is supported at point H about which it is on the verge of rotation. The rectangular abutment has height b and width y.

Figure 2a shows the forces acting that arise from weight. In terms of area, the weight of the abutment is the product of b and y, and the weight of the part of the arch below ML and above the abutment is denoted by A'. These weights act through their respective centers of gravity P and K, located by the dimensions $\frac{y}{2}$ and $\frac{y}{2}+h$, respectively. The weight A of the half arch segment above ML acts normal to joint ML in the amount $A/\sin(\theta)$, as discussed previously. The point of application of the thrust $A/\sin(\theta)$ is at L on the intrados. The abutment width y is the desired quantity to be determined.

De la Hire visualizes the part shown in Figure 2a as a bent lever, which is depicted by the heavy line LHT in Figure 2b. The fulcrum is point H, and the ends of the lever where loads are applied are point T at mid-point of the base of the abutment and point L. The load on T is downward and comes from the weights by and A'. Because the line of action of weight A' does not pass through T, de la Hire adjusts A' by a factor of $\left(\frac{y}{2}+h\right)/\left(\frac{y}{2}\right)$, which gives the same moment about H when applied at T. Thus, the total force on the lever at T is $by+(1+\frac{2h}{y})A'$.

At point L of the lever, as shown in Figure 2b, de la Hire resolves the thrust into component D perpendicular to the lever arm LH and another component (not labelled in the figure) parallel to LH. In this way, only D needs to be considered in moment equilibrium of the lever. Thus,

$$D\cdot\overline{LH}=\left[by+\left(1+\frac{2h}{y}\right)A'\right]\cdot\frac{y}{2}, \quad (1)$$

where the overbar denotes length.

The rest of the derivation makes use of Figure 1. Point C is on the intersection of the continuation of joint line ML and the centerline. Line LG is perpendicular to the lever arm LH. Line GR is perpendicular to line LC. Line LJ is perpendicular to joint line ML, and so it is on the line of action of the thrust. Angle JHL is a right angle. Lengths y, a, b, g, e and f are as

labelled in the figure. Some shortcuts will be taken below compared to de la Hire's derivation, but the result will be the same.

Triangles LJH and LGR in Figure 1 are similar. Let line LJ represent the thrust $A/\sin(\theta)$, then line JH represents force D. By similar triangles,

$$\frac{D}{A/sin\theta} = \frac{\overline{GR}}{\overline{LG}} \ , \quad (2)$$

where $\overline{GR} = \overline{GC}\sin(\theta)$. Triangles LHA and LGE are also similar, so $\overline{LG} = \overline{LH}\frac{f}{g}$ and $\overline{GC} = e - \overline{EG} = e - \frac{f}{g}(y + a)$. Substitution into Equation 2 gives

$$D \cdot \overline{LH} = A\left(\frac{eg}{f} - y - a\right). \quad (3)$$

A further substitution into Equation 1 and grouping terms leads to

$$\frac{1}{2}by^2 + \left(\frac{1}{2}A' + A\right)y + A'h - Ag\frac{e}{f} + Aa = 0 \ , \quad (4)$$

which is quadratic in y. Equation 4 is the same as de la Hire's equation after dividing the latter through by f.

In de la Hire's treatment, he states that the weight A of the half arch above joint ML acts vertically on point L (which is confusing since he neglects to mention the horizontal component of the thrust), and then he says one knows from mechanics that $D{:}\,A = \overline{GC}{:}\,\overline{LG}$. Although he does not detail the process used to obtain this relation, it is equivalent to Equation 2.

Instead of dealing with Equation 4, de la Hire makes a simplification and replaces the weight A' by extending the rectangular abutment up to the level of point L, keeping the same abutment width y and the same horizontal position. Thus, A' in Equation 4 is set to zero and b is replaced by g:

$$\frac{1}{2}gy^2 + Ay - Ag\frac{e}{f} + Aa = 0 \ . \quad (5)$$

According to the quadratic formula, the solution for the simplified geometry is given by

$$y = -\frac{A}{g} \pm \left(\frac{A^2}{g^2} + 2A\frac{e}{f} - 2A\frac{a}{g}\right)^{\frac{1}{2}}. \quad (6)$$

So, when $\frac{e}{f} > \frac{a}{g}$, Equation 6 has one positive and one negative root, and the positive one is the desired abutment width y (+ sign for the radical). No explicit factor of safely is included by de la Hire.

Nowhere in the derivation has any specific value been used for θ. Thus, a conclusion by others that de la Hire's solution only applies for $\theta = 45^{\circ}$ [6] seems to be incorrect.

Worth noting is that Equation 4 is not solvable because h as it is defined in Figure 2a is a function of y. This is not an issue for de la Hire because he focuses on Equation 5, but Equation

4 can be reformulated using an alternative to h (Figure 2c). The moment arm for the weight A' about point H is $r_i + y - h'$, where r_i is the radius of the intrados and h' is the horizontal distance of the center of gravity of A' from the centerline given by

$$h' = \frac{1}{3A'}(r_e^3 - r_i^3)\sin\left(\frac{\pi}{2} - \theta\right). \quad (7)$$

Use of the new expression for the moment arm of A' results in

$$\frac{1}{2}by^2 + A_{\text{half}}\, y + A'r_i - A'h' - Ag\frac{e}{f} + Aa = 0\,, \quad (8)$$

which replaces Equation 4 and where $A_{\text{half}} = A' + A$ is the weight of the complete half arch, not a function of θ.

The solutions for abutment width y from Equation 5 (simplified geometry) and Equation 8 (actual geometry) are compared in Figure 4, using the dimensions listed in the caption of Figure 1. These dimensions approximate de la Hire's geometry shown in Figure A1. In Figure 4, both abutment widths are shown as functions of the angle θ that locates the joint. In each case, the abutment width increases monotonically as θ reduces, and greater width occurs for the case with the simplified geometry for a given value of θ. Thus, the choice of joint position angle θ makes a difference, as does the choice of Equation 5 or 8. For θ = 45º, y = 31.7 units (simplified geometry) and y = 29.3 units (actual geometry), a difference of about 8%. The dashed line in the figure marks a possible lower bound on the abutment width, taken as the arch thickness $r_e - r_i$ = 25 units, which could be imposed by architectural considerations.

4. GRAPHICAL CONSTRUCTION TO DETERMINE ABUTMENT WIDTH FOR THE CIRCULAR ARCH

Benvenuto [5] claims that de la Hire's quadratic equation for abutment width in the case of the circular arch and the accompanying graphical construction give "quite different results". He also describes the graphical construction (Figure A2) as a "welter of lines, segments, circles and arcs" and as a "tangle of points and segments." The point Benvenuto makes is that the complexity of the graphical construction and the discrepancy with the theory led to confusion at the time, with the implication that it impeded acceptance of the scientific methods. Benvenuto says that "not surprisingly, the contradiction has never been clarified." Whether or not this last statement was or is still true, no analysis of de la Hire's graphical constructions, either for the circular arch or for the plate-bande (discussed later in Section 6) could be located.

Benvenuto is correct in pointing out a discrepancy between de la Hire's equation for abutment width and his graphical solution. Below, a corrected version of de la Hire's graphical construction is explained first, and then the error is identified and assessed.

Figure 5 is a graphical evaluation of Equation 6 for the positive root, which is the abutment width y. It corresponds to a corrected version of de la Hire's construction shown in Figure A2. The solid lines are drawn during the graphical solution, and the dotted lines show the half arch and one abutment for reference. The dimensions used for Figure 5 are the same as those listed in the caption of Figure 1, which approximately match de la Hire's geometry. The angle θ for the joint ML is taken to be 45º. Figure 5 has been drawn with the computer, so there are no drafting errors.

The step-by-step process is given below, interspersed with some explanations.

1. Compute area A of the half arch segment above the joint ML and its square root $\sqrt{A}$.

De la Hire does not discuss this step, but for a circular arch of constant thickness, $\sqrt{A}$ is proportional to $(r_e^2 - r_i^2)^{\frac{1}{2}}$, which can be easily found graphically, and where r_e and r_i are the radii of the extrados and intrados, respectively.

2. Plot points M, L, S and F and the vertical centerline through F.

M and L should define a radial joint at the desired angle θ from the centerline.

3. Locate point C where a line through M and L intersects the centerline.
4. Locate point E where a horizontal line through L intersects the centerline.
5. Locate point A where a vertical line downward from L intersects a horizontal line from S.

The lengths $\overline{LE}$, $\overline{EC}$, $\overline{LA}$ and $\overline{SA}$ are denoted by f, e, g and a, respectively.

6. Locate point X on an extension of line LE so that $\overline{LX} = \sqrt{A}$.
7. Locate point Z on line LA so that $\overline{LZ} = \sqrt{A}$.
8. Locate point 4 on line LA by drawing line ZE and then drawing line $4X$ parallel to it.

Using the similar triangles LZE and $L4X$, $\overline{L4}{:}\overline{LX} = \overline{LZ}{:}\overline{LE}$, and thus $\overline{L4} = \frac{A}{f}$.

9. Locate point Y on line LE by drawing line AE and then drawing line $4Y$ parallel to it.

Using the similar triangles $L4Y$ and LAE, $\overline{LY}{:}\overline{L4} = \overline{LE}{:}\overline{LA}$, and thus $\overline{LY} = \frac{A}{g}$.

10. Locate point Q where a line from C drawn perpendicular to line AE intersects a horizontal extension of the line LE.

Using the similar triangles EQC and LAE, $\overline{QE}{:}\overline{LA} = \overline{EC}{:}\overline{LE}$, and thus $\overline{QE} = \frac{eg}{f}$.

11. Locate point 7 on a horizontal extension of line LE by making the length of line $L7$ equal to $\overline{QE} - \overline{SA}$.

Thus, $\overline{L7} = \frac{eg}{f} - a$.

12. Locate point 6 on the line LE extension so that $\overline{6L} = \overline{LY}$.

Thus, $\overline{6L} = \frac{A}{g}$.

13. Locate point 8 where line LA intersects a circular arc with center at point 7 and drawn through point 6.

Consider point 6′ one radius of the arc to the right of point 7. (De la Hire does not mention this point, and it does not have to be plotted.) Thus, $\overline{L6'} = \overline{6L} + 2 \cdot \overline{L7} = \frac{A}{g} + 2\frac{eg}{f} - 2a$. Using the similar triangles $L86$ and $L6'8$ (neither drawn in the figure), $\overline{L8}: \overline{6L} = \overline{L6'}: \overline{L8}$, thus $\overline{L8} = \left(\frac{A^2}{g^2} + 2A\frac{e}{f} - 2A\frac{a}{g}\right)^{\frac{1}{2}}$.

14. Locate point 9 on the line LA so that $\overline{L9} = \overline{LY}$.

Thus, $L9 = A/g$. The length of line 98 is equal to $\overline{L8} - \overline{L9}$, thus $\overline{98} = -\frac{A}{g} + \left(\frac{A^2}{g^2} + 2A\frac{e}{f} - 2A\frac{a}{g}\right)^{\frac{1}{2}}$. This is equal to the abutment width y given by Equation 6 after adjustment by whatever scale is being used for the plot.

The above construction is the same as de la Hire's except for Step 11 where de la Hire sets the length of $L7$ to $\frac{1}{2}\overline{LY} + \overline{QE} - \overline{SA} = \frac{1}{2}\frac{A}{g} + \frac{eg}{f} - a$. This mistake moves point 7 to the right, increasing the radius of the arc. The result is that point 8 moves down, which increases the length of line 98, i.e., the abutment width. Thus, the error is conservative.

The insert in Figure 5 compares the corrected graphical solution (solid line) with de la Hire's graphical solution (dashed line). The increase in abutment width for the latter is slight for the particular geometry employed, about 4%, not "quite different" as Benvenuto [5] states. But the error could be somewhat greater for a different selection of parameters. If de la Hire had solved Equation 6 analytically and compared the resulting abutment width to that from his graphical solution, which he might have done, the small difference may not have suggested that the graphical solution contained an error.

5. DE LA HIRE'S CIRCULAR ARCH WITH FRICTION INCLUDED

As mentioned previously, de la Hire's solution for the circular arch is consistent with a collapse mechanism in which the top portion of the arch slides down and the abutments rotate out, as shown in Figure 3. His solution applies to the case where the inclined joints in the arch are frictionless. Even though de la Hire was familiar with the concept of friction, he neglects to even mention it in his Memoir. It is of interest here to include the effect of friction in order to see what difference it makes in two respects: How difficult is it to include friction? How much does it affect the results?

Before beginning, another aspect of de la Hire's solution needs to be discussed. He assumes that the central part of the arch between the two inclined joints remains as a single solid piece, same for each side below the joints. This assumption requires the presence of strong grout between the joints of the stones within the three solid pieces so that separation and sliding do not occur there. Since grout, if used, often had questionable quality, a more conservative approach would be to neglect its effect. Therefore, two models are considered here. First is the *three-piece model* as analyzed by de la Hire, but now including friction. In the second model, separation without tensile resistance and sliding with frictional resistance are possible at any radial joint in the arch. To facilitate the mathematics, the joint spacing in the arch is taken to be infinitesimal. This model is referred to as the *continuum model*.

Both these analyses are made for de la Hire's circular arch shown in Figure 1. The actual geometry, i.e., using weight A' rather than the extended abutment, is employed.

Three-piece model

Inclusion of friction alters both the magnitude and direction of the force acting at point L as shown in Figure 6 for the circular arch. The addition of a friction force component parallel to the joint ML changes the direction of the thrust from normal to the joint to having an angle ϕ with respect to the joint. To maintain vertical equilibrium of the central portion of the arch, the magnitude of the thrust becomes $A/\sin(\theta+\phi)$. The angle ϕ is the friction angle, where $\tan(\phi)$ equals the friction coefficient μ.

Instead of resolving the thrust $A/\sin(\theta+\phi)$ into components along and perpendicular to de la Hire's lever arm LH, the moment about point H will be taken using $A/\sin(\theta+\phi)$ itself and the perpendicular distance $\overline{UH}$. The dotted line in Figure 6 from point L through point U is on the line of action of $A/\sin(\theta+\phi)$. Using some geometrical substitutions based on the figure:

$$\frac{A}{\sin(\theta+\phi)} \cdot \overline{UH} = A \cdot t = A\left(\frac{g}{\tan(\theta+\phi)} - y - a\right). \quad (9)$$

This expression substitutes for the one in Equation 3, and thus inclusion of friction replaces $\frac{e}{f}$ with $\frac{1}{\tan(\theta+\phi)}$. So, Equation 8 is modified to:

$$\frac{1}{2}by^2 + A_{\text{half}}\, y + A'r_i - A'h' - A\frac{g}{\tan(\theta+\phi)} + Aa = 0. \quad (10)$$

As seen, including friction involves only a minor adjustment to the previous formulation.

The abutment width from Equation 10 using de la Hire's geometry (see caption of Figure 1 for dimensions) and θ equal to 45º is plotted in Figure 7 as a function of μ over the range from 0 to 1. The value at μ = 0 (y = 29.3 units) agrees with the result from Equation 8. As seen in the figure, friction causes a significant reduction in y, even for low values of μ. The presumed architectural lower bound of $r_e - r_i$ = 25 units (dashed line in the figure) controls over practically all the friction range.

Continuum model

The results below for the continuum model were obtained by a computerized process that examined many mechanisms of collapse and their dependence on locations of sliding planes and hinging joints and on the coefficient of friction. This process was conducted using the dimensions listed in the caption of Figure 1. For a different geometry, the set of mechanisms identified could be different.

For wide, stable abutments, De la Hire's cylindrical arch will collapse by sliding if the coefficient of friction μ is less than or equal to 0.309. When μ = 0.309, the mechanism involves two pairs of sliding planes, as shown in Figure 8a. When the ratio of the normal force to the friction force at the base of the arch (top of abutment) equals 0.309, the peak value of this ratio for joints above the base is also 0.309, and this joint occurs at θ_S= ±28.6º. Thus, the base of the arch and this joint are the sliding planes. A line of thrust can be found which is contained entirely within the arch. When μ exceeds 0.309, only the pair of inclined sliding planes stays active, and so the collapse mechanism shown in Figure 8a stabilizes.

When μ exceeds 0.309, and for narrow enough abutments, a collapse mechanism of the type shown in Figure 8b occurs, consisting of an inclined sliding plane and a hinging joint on each side of the arch with the abutments rotating about their outside base corners. The three parameters of the mechanism are all functions of the friction coefficient μ: the angle θ_S of the sliding joint, the angle θ_H of the hinging joint, and the abutment width y. They are shown in Figure 8b for values of these parameters corresponding to μ = 0.60, and in Figure 9 as functions of μ (between values of 0.309 and 0.915). No rotation occurs for the portion of the arch between the hinging joint and the sliding plane. The line of thrust lies within the arch except where it touches the intrados at θ_H, allowing the hinge to form. The relatively narrow abutment width is

necessary to develop the hinge at the base of the abutment. For a given value of μ, an abutment width exceeding the value of y given in Figure 9 stabilizes the structure.

At μ = 0.915, the sliding planes becomes inactive and another hinge forms in the arch at the crown where the line of thrust reaches the extrados. A five-hinge collapse mechanism (Figure 8c) is present for μ exceeding 0.915, which is unaffected by the value of μ. This is reflected in Figure 9 by the constant values for θ_H and y for μ exceeding 0.915. An abutment wider than this value of y stabilizes the structure.

The dashed line in Figure 9 again represents the presumed architectural lower bound on abutment width, equal to the arch thickness. A comparison of Figure 7 (three-piece model) with Figure 9 (continuum model) reveals smaller abutment widths for the former for the same friction coefficient.

The series of mechanisms described above do not include the type shown in Figure 3 in which the same joint accommodates both hinging and sliding. In a continuum model, the hinging joint coinciding with the sliding joint (where the ratio of friction force to normal force reaches a maximum along the arch) would be unusual.

6. PLATE-BANDE

Shown in Figure 10 is the geometry of de la Hire's plate-bande, with the thickness of the plate-bande denoted by t and its half span by f. The height of the abutment is now denoted by g, which is consistent with its usage for the circular arch as the vertical distance from the base of the abutment to point L (see Figure 1). The pair of joints ML is located adjacent to the abutments, and θ_{pb} denotes their angle from vertical, with their extended planes passing through point C. The three pieces separated by the joints ML are considered to be solid, and the weights $NBLM$ atop the abutments are neglected, which de La Hire justifies as being conservative. Thrusts at the joints are in the normal direction, consistent with neglecting friction. Horizontal displacement at the base of the abutments is restrained.

With the weights $NBLM$ neglected, the equation to determine abutment width for the plate-bande can be obtained as a special case of Equation 5 for the circular arch by setting length a (refer to Figure 1) to zero. Thus,

$$\frac{1}{2}gy^2 + Ay - Ag\frac{e}{f} = 0, \quad (11)$$

where A is the weight of $MLEF$. Equation 11 is the same as de la Hire's equation after multiplying the latter through by $\frac{g}{2}$. However, de la Hire derives the relation from scratch, never

mentioning that it is a special case of Equation 5. He says only that "ce cas n'est pas tout-à-fait si composé que le precedent", meaning the plate-bande is simpler than the circular arch.

The omitted weights $NBLM$ can be included with some effort, noting that this weight is a function of y. The result is

$$\left(\frac{1}{2}g + \frac{1}{2}t\right)y^2 + ft\,y + \frac{1}{2}f^2t - Af + Ah_A - Ag\frac{e}{f} = 0, \quad (12)$$

still quadratic in y, where h_A is the horizontal distance from the centerline to the center of gravity of weight A equal to

$$h_A = \frac{tf^2}{2A}\left(1 + \frac{t}{e} + \frac{1}{3}\frac{t^2}{e^2}\right). \quad (13)$$

Using the dimensions listed in the caption of Figure 10, which approximately match de la Hire's geometry in Figure A3, the abutment widths given by Equation 11 (weight $NBLM$ omitted) and Equation 12 (weight $NBLM$ included) are 60.4 units and 55.7 units, respectively. This difference is about 8%. For reference, the plate-bande thickness is 29 units.

The graphical construction to determine the abutment width y for the plate-bande is shown in Figure 11 (produced by computer), which corresponds to de la Hire's construction shown in Figure A3. The solid lines are drawn during the solution, and the dotted lines show the half plate-bande and one abutment for reference. The dimensions used for Figure 11 are those from the caption of Figure 10, which approximately match de la Hire's geometry. This solution is for weights *NBLM* omitted (Equation 11).

The step-by-step process in the graphical solution is given below, interspersed with some explanations.

1. Plot points M, L, S and F and the vertical centerline (through F).
2. Locate point C where a line through M and L intersects the centerline.
3. Locate point E where a horizontal line through L intersects the centerline.

The lengths $\overline{LE}$, $\overline{EC}$, $\overline{LS}$ and $\overline{FE}$ are denoted by f, e, g and t, respectively.

4. Locate point 7 on the line ML midway between points M and L.
5. Locate point 3 where a horizontal line through point 7 intersects the centerline.

The length of the line 73 equals $\frac{A}{t}$, where A is the area of the plate-bande segment $MLEF$.

6. Locate point 10 on the centerline so that $\overline{E10} = \overline{73}$.

Thus, $\overline{E10} = \frac{A}{t}$.

7. Locate point 11 where line LE intersects a circular arc with center midway between points F and 10 and with radius equal to $\frac{1}{2}\overline{F10}$.

Using the similar triangles $E11F$ and $E10\ 11$ (neither drawn in the figure), $\overline{11E}:\overline{FE} = \overline{E10}:\overline{11E}$, and thus $\overline{11E} = \sqrt{A}$.

8. Locate point 12 on the line LE so that $\overline{L12} = \overline{11E}$.

Thus, $\overline{L12} = \sqrt{A}$.

9. Locate point 15 on the line FE so that $\overline{15E} = \frac{1}{2}\overline{LE}$.

Thus, $\overline{15E} = \frac{f}{2}$.

10. Locate point 16 where line LE intersects a circular arc with center midway between points 15 and C and with radius equal to $\frac{1}{2}\overline{15C}$.

Using the similar triangles $E16\ 15$ (not drawn in figure) and $EC16$, $\overline{16E}:\overline{15E} = \overline{EC}:\overline{16E}$, and thus $\overline{16E} = \sqrt{\frac{ef}{2}}$.

11. Locate point 13 on the line drawn vertically upward from point L by drawing line $S12$ and then drawing line 13 12 perpendicular to it through point 12.

Using the similar triangles $13L12$ and $12LS$, $\overline{13L}:\overline{L12} = \overline{L12}:\overline{LS}$, and thus $\overline{13L} = \frac{A}{g}$.

12. Locate point 18 on the centerline by drawing line $16C$ and then drawing line 11 18 parallel to it.

Using the similar triangles $E18\ 11$ and $EC16$, $\overline{E18}:\overline{11E} = \overline{EC}:\overline{16E}$, and thus $\overline{E18} = \sqrt{\frac{2Ae}{f}}$.

13. Locate point 19 on a horizontal extension of line LE by making the length of line $E19$ equal to $\overline{13L}$.

Thus, $\overline{E19} = \frac{A}{g}$. Since $E18\ 19$ is a right triangle, $\overline{18\ 19} = (\overline{E19}^{\,2} + \overline{E18}^{\,2})^{\frac{1}{2}} = \left(\frac{A^2}{g^2} + 2A\frac{e}{f}\right)^{\frac{1}{2}}$.

14. Locate point 9 on the line 18 19 by making the length of line 9 19 equal to $\overline{13L}$.

Thus, $\overline{9\ 19} = \frac{A}{g}$. The length of line 18 9 is equal to $\overline{18\ 19} - \overline{9\ 19}$, thus $\overline{18\ 9} = -\frac{A}{g} + \left(\frac{A^2}{g^2} + 2A\frac{e}{f}\right)^{\frac{1}{2}}$. This is the abutment width y resulting from Equation 11 after adjustment by whatever scale is being used for the plot.

De la Hire's graphical construction for the plate-bande therefore seems to be correct. However, the question arises as to why he devised a different and more complicated graphical construction for the plate-bande since Equation 11 is a special case of Equation 5 for the circular arch. Indeed, the graphical solution described in Section 4 works for the plate-bande, as shown in Figure 12. De la Hire must have recognized this special case relationship, if not before he derived the equation for abutment width of the plate-bande, then surely afterwards. There may be some advantages one to the other regarding the accuracy to which the graphical constructions can be made, but such are not obvious. De la Hire was a geometrician and published on the subject [12], so presumably he was well versed in such things.

7. DE LA HIRE'S PLATE-BANDE WITH FRICTION INCLUDED

As with the circular arch, it is of interest here to include the effect of friction for the plate-bande in order to see what difference it makes. Both a three-piece model and a continuum model of the plate-bande shown in Figure 10 are investigated. The actual geometry, i.e., with weight $NBLM$ included, is employed. For the continuum model, the joints of infinitesimal spacing are oriented so their extended planes all pass through point C.

Three-piece model

For the three-piece model, repeating what was done for the circular arch in Section 5, inclusion of friction replaces $\frac{e}{f}$ with $\frac{1}{\tan(\theta+\phi)}$ in Equation 12. Thus,

$$\left(\frac{1}{2}g+\frac{1}{2}t\right)y^2+fty+\frac{1}{2}f^2t-Af+Ah_A-A\frac{g}{\tan(\theta+\phi)}=0. \quad (14)$$

The width y from Equation 14 using de la Hire's geometry (dimensions listed in the caption to Figure 10) is plotted in Figure 13 as a function of μ over the range from 0 to 1. The value at μ = 0 (y = 55.7 units) agrees with the result from Equation 12. As seen, friction causes a significant reduction in y.

Continuum solution

As with the circular arch, the continuum model of the plate-bande was analyzed by a computerized process that examined many mechanisms of collapse and their dependence on locations of sliding planes and hinging joints and on the coefficient of friction. This process used the specific dimensions listed in the caption of Figure 10. For a different geometry, the set of mechanisms identified could be different.

An addition assumption made in the continuum solution is that sliding is prevented from occurring along the joint BL at the top of each abutment. Depending on the coefficient of friction, this could require keyed construction.

For narrow enough abutments, two collapse mechanisms can occur depending on the coefficient of friction μ, as shown in Figure 14. In part a, both hinging and sliding occur at the same location (joint ML), which is something that did not happen with the circular arch. Hinging also occurs at the base of the abutments as they rotate out. This mechanism is the same as what occurs for the three-piece model, and no intermediate joint in the plate-bande is involved. Thus, the equation for abutment width y is the same as given by Equation 14, and this equation applies in the range of μ from zero to 0.444. The abutment width in Figure 14a is shown for μ = 0.30. For μ above 0.444, the mechanism in Figure 14b occurs. This is a five-hinge mechanism; sliding ceases along joint ML, and the crown becomes a hinge point. The abutment width y is independent of the value of μ. The variation of y as a function of μ is shown in Figure 15 for the range of μ from 0 to 1. Abutment widths wider than shown in Figure 15 for a given value of μ stabilize the structure.

8. SUMMARY

The conclusion by others [5-8] that de la Hire based his analysis on a collapse mechanism involving the central part of the arch acting as a wedge, rotating the abutments outward as it drops, does not seem to be justified. Although such a mechanism is consistent with de la Hire's analysis, his writing lacks enough detail to support this view, which, if true, would make de la Hire not only a pioneer of static analysis of structures but a pioneer of limit analysis as well.

De la Hire's derivation of the quadratic equation for the abutment width of the circular arch, which uses a three-piece structural model, is general in terms of the position angle of the pair of inclined joints in the arch, a conclusion contrary to that reached by others [6].

De la Hire's construction for finding the abutment width for a circular arch by graphically solving the associated quadratic equation contains an error, as suspected by another writer [5]. This error has a minor effect on the results, as least for the particular arch geometry employed. A different graphical construction used by de la Hire for the plate-bande appears to be correct. However, given that the plate-bande solution is a special case of the one for the circular arch, the plate-bande graphical construction seems to be needlessly complicated and unnecessary, or at least its advantage is not evident.

Friction can be included in de la Hire's three-piece structural models quite easily. For a continuum model, where hinging or sliding can take place anywhere along the arch or plate-

bande, the situation is more complicated. Different collapse mechanisms occur depending on the value of the coefficient of friction. Generally, higher coefficients of friction make the structure more stable when the collapse mechanism involves sliding, so the required abutment widths are smaller. For the circular arch that de la Hire analyzed, an abutment width equal to the arch thickness, which could be considered as an architectural lower bound, is satisfactory for realistic values of the friction coefficient.

9. REFERENCES

1. Philippe de la Hire, *Traité de Mécanique ou l'on explique tout ce qui est nécessaire dans la pratique des Arts, et les propriétés des corps pesants lesquelles ont un plus grand usage dans la Physique*, A Paris de l'Imprimerie Royale, 1695.

2. Philippe de la Hire, Sur la construction des voûtes dans les édifices, *Mémoires de Mathématique et de Physique*, tirés des Registres de l'Académie Royale des Sciences, Paris, 1712, pp 69-77.

3. Correspondent, Some account of the different theories of arches or vaults, and of domes, and of the authors who have written on this most delicate and important application of mathematical science, *The Philosophical Magazine Comprehending the Various Branches of Science, the Liberal and Fine Arts, Geology, Agriculture, Manufactures and Commerce,* Alexander Tilloch, London, Vol. 38, 1811, pp 387-391, 409-420.

4. Jacques Heyman, *Coulomb's Memoir on Statics, An Essay in the History of Civil Engineering*, Cambridge University Press, Cambridge, 1972.

5. Edoardo Benvenuto, *An Introduction to the History of Structural Mechanics Part II: Vaulted Structures and Elastic Systems*, Springer-Verlag, New York, NY, 1991 (originally published in Italian by G. C. Sansoni, 1981).

6. A. Buti and M. Corradi, I contributi di un matematico del XVII secolo ad un problema di architettura: Philippe de la Hire e la statica degli archi, *Atti della Accademia Ligure di Scienze e Lettere*, Genoa, Vol. 38, 1982, pp 303-323.

7. Anna Sinopoli, A re-examination of some theories on vaulted structures: the role of geometry from Leonardo to de La Hire, *Towards a History of Construction: Dedicated to Edoardo Benvenuto* (edited by Antonio Becchi, Massimo Corradi, Federico Foce and Orietta Pedemonte), Birkhaüser, 2002, pp 601-624.

8. Karl-Eugen Kurrer, *The History of the Theory of Structures: From Arch Analysis to Computational Mechanics*, Ernst & Sohn Verlag für Architektur und technische Wissenschaften GmbH & Co. KG, Berlin, 2008.

9. Santiago Huerta, The safety of masonry buttresses, *Proceedings of the Institute of Civil Engineers, Engineering History and Heritage*, Vol 163, 2010, pp 3-24.

10. C. Stewart Gillmor, *Coulomb and the Evolution of Physics and Engineering in Eighteenth-Century France*, Princeton University Press, Princeton, New Jersey, 1971.

11. Bernard Forest de Belidor, *La Science des Ingenieurs dans la Conduite des Travaux de Fortification et d'Architecture Civile*, Claude Jombert, Paris, 1729.

12. Philippe de la Hire, *Sectiones Conicae in Novem Libros Distributae*, Michallet, Paris, 1685.

10. FIGURES

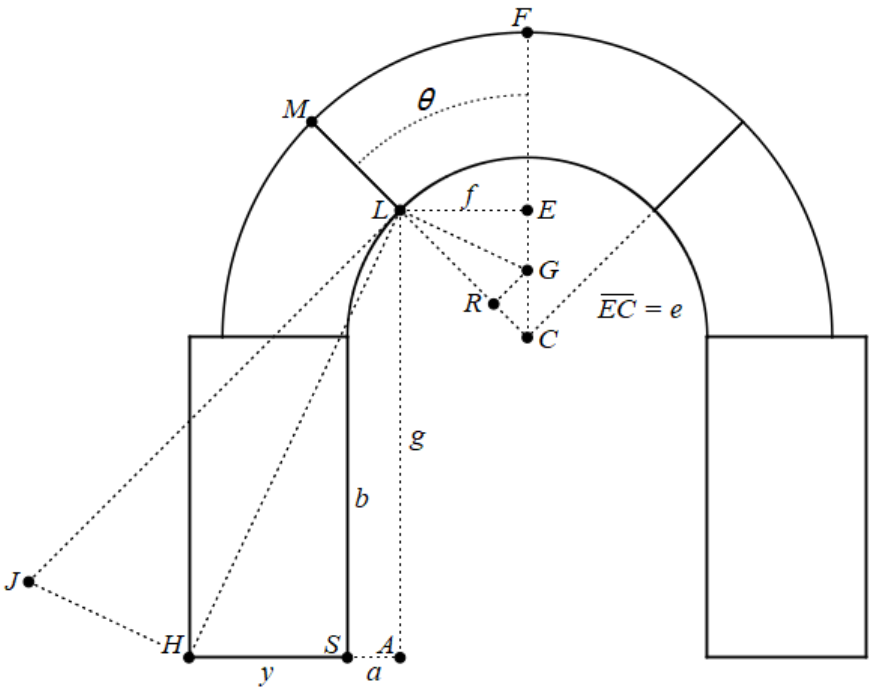

Figure 1. Version of Figure A1 showing the circular arch together with lines and labels used to derive the equation for abutment width. Dimensions in arbitrary units as scaled from Figure A1 are $\overline{MC}$ = 61 (radius r_e of extrados), $\overline{LC}$ = 36 (radius r_i of intrados) and b = 64 (height of abutment).

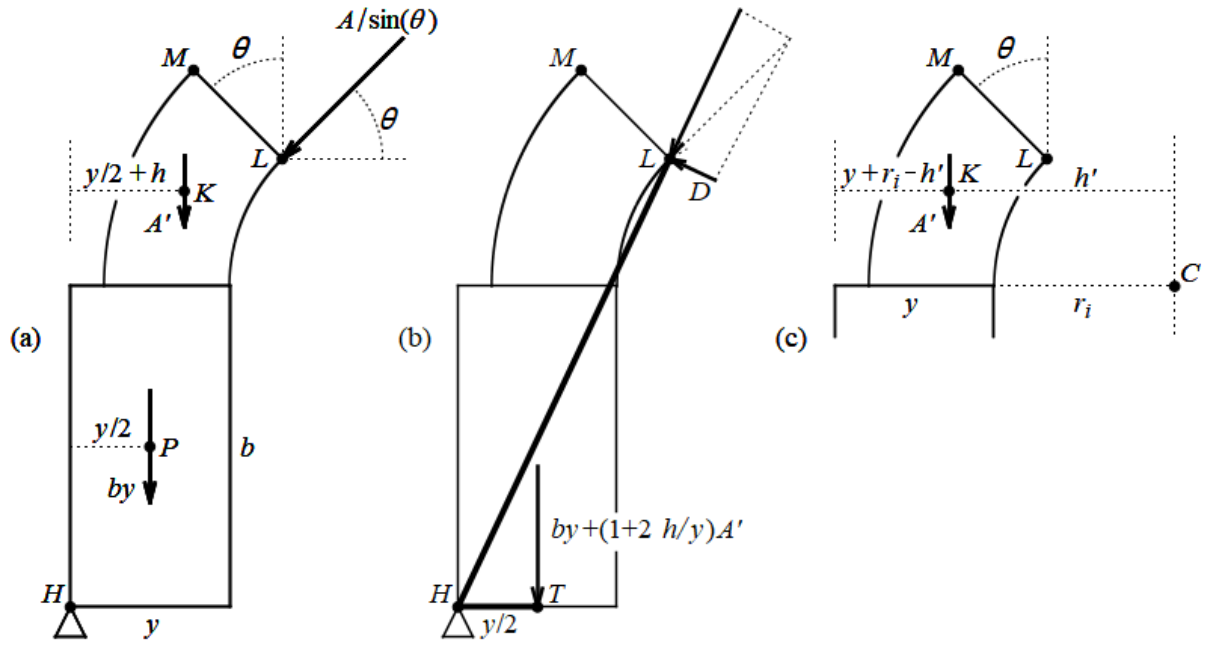

Figure 2. Aid to de la Hire's derivation of equation for abutment width for the circular arch, showing one side of the arch below the joint, including abutment and its hinge point. Part (a): Forces acting. Part (b): Use of bent lever LHT with fulcrum at abutment hinge point H. Part (c): Alternative dimensioning for the center of gravity of weight A' used to derive Equation 8.

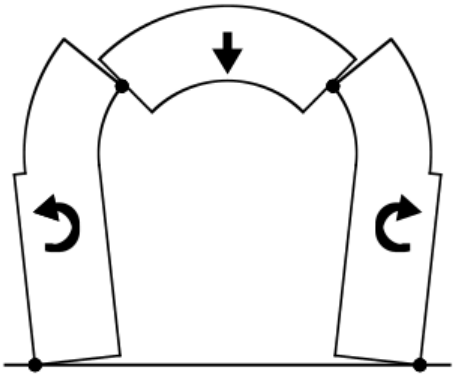

Figure 3. Collapse mechanism attributed to de la Hire [5-8], involving rotation of the abutment levers and sliding down of the arch wedge.

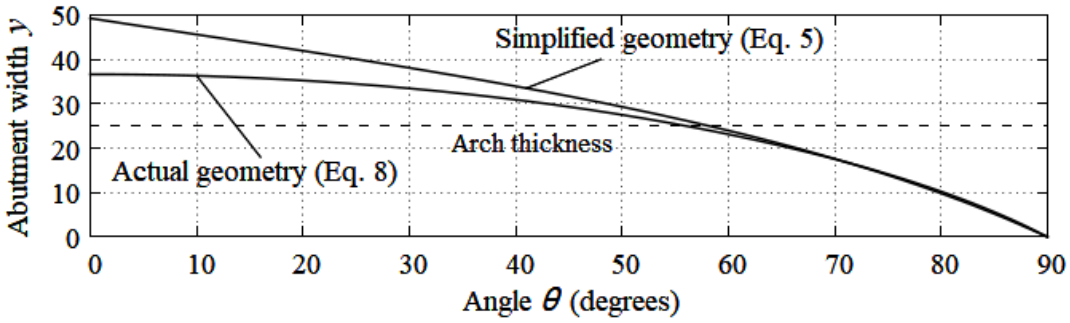

Figure 4. Abutment width for de la Hire's analysis of his circular arch as a function of joint position angle θ: comparison of Equation 5 (simplified geometry) and Equation 8 (actual geometry).

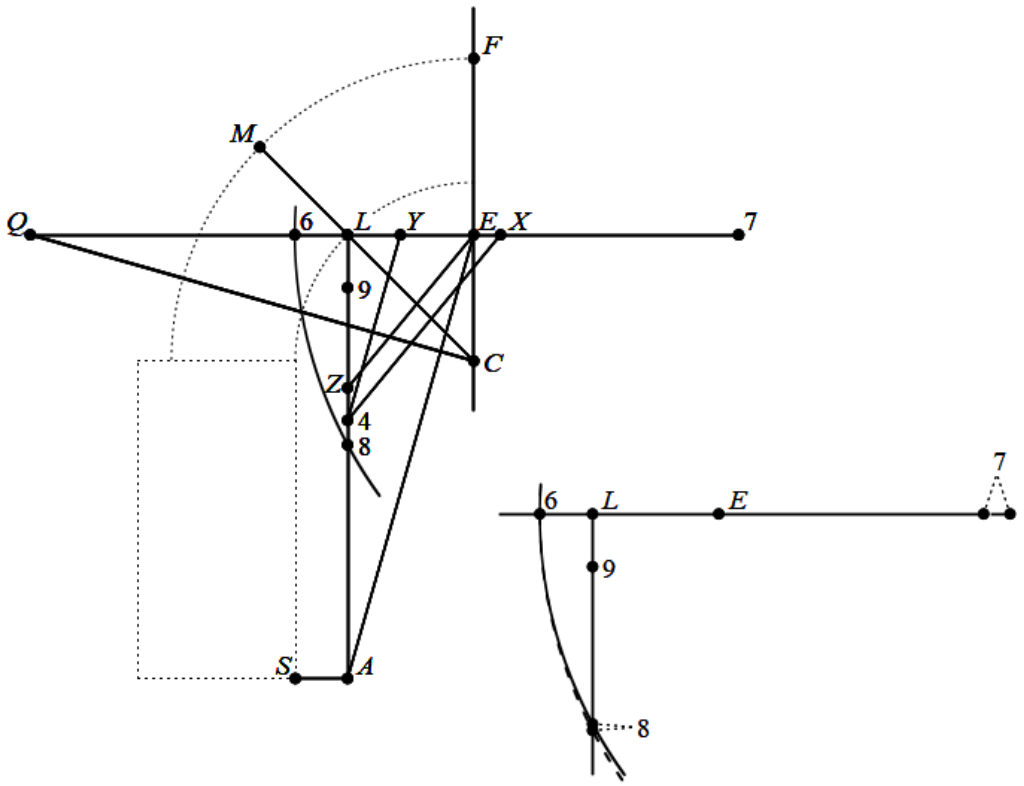

Figure 5. Version of Figure A2 showing the graphical construction to determine abutment width for the circular arch. The angle θ for the joint ML equals 45°. Length of line 98 is the desired abutment width. The main diagram above shows the corrected version of de la Hire's construction, and the dashed arc in the insert is drawn with de la Hire's error.

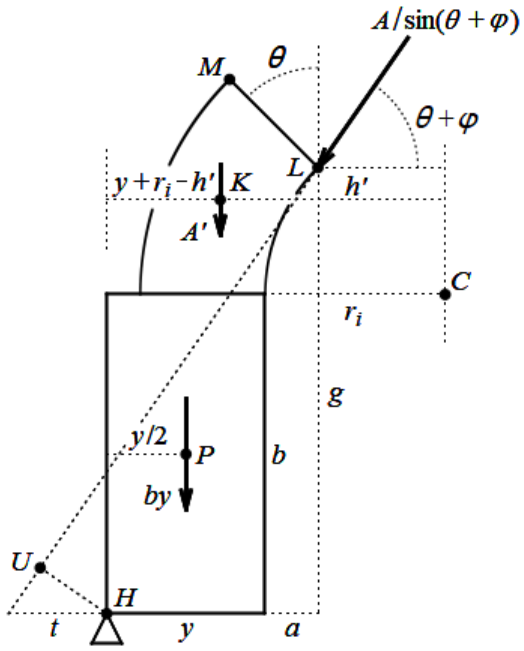

Figure 6. Aid to derivation of Equation 10 for abutment width (three-piece circular arch with friction included).

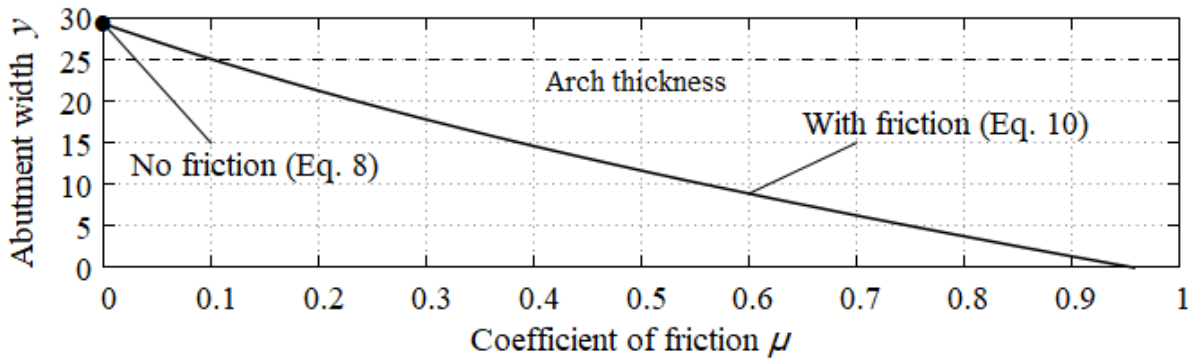

Figure 7. Abutment width predicted by Equation 10 for de la Hire's circular arch (actual geometry) over a range of the friction coefficient μ from 0 to 1. De la Hire's no-friction solution from Equation 8 is marked. This plot is for the three-piece model with joint ML located at θ equal to 45º.

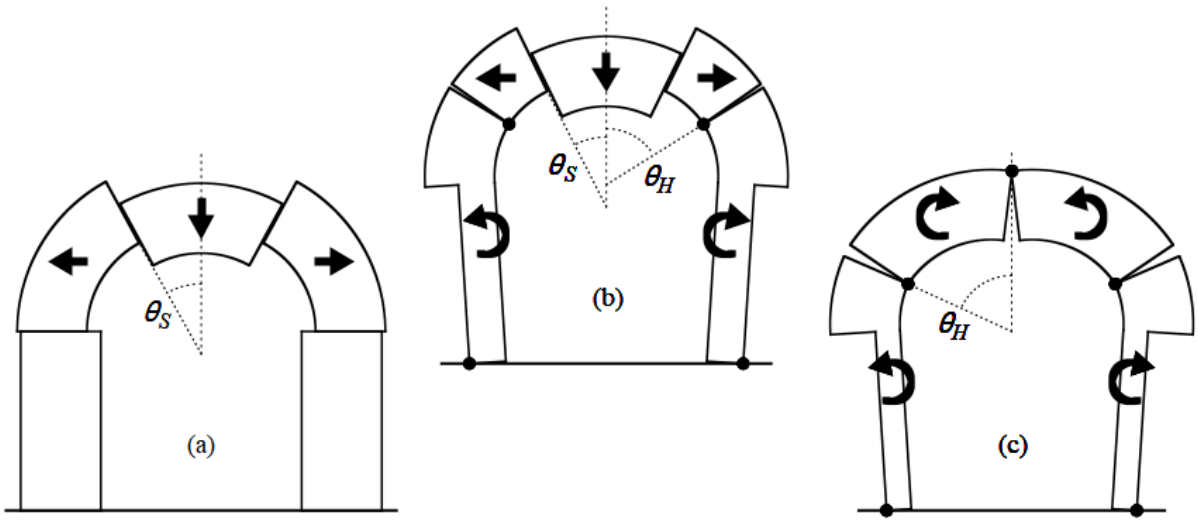

Figure 8: The three collapse mechanisms that occur in a continuum model of de La Hire's circular arch, depending on the value of the coefficient of friction μ. Mid-arch hinging joints are located with θ_H, and mid-arch sliding planes are located with θ_S. Dots denote hinge points. Part (a): two pairs of sliding planes; the wide abutment is stationary. Part (b): Four hinge points and two sliding planes. Part (c): Hinging only; no sliding planes.

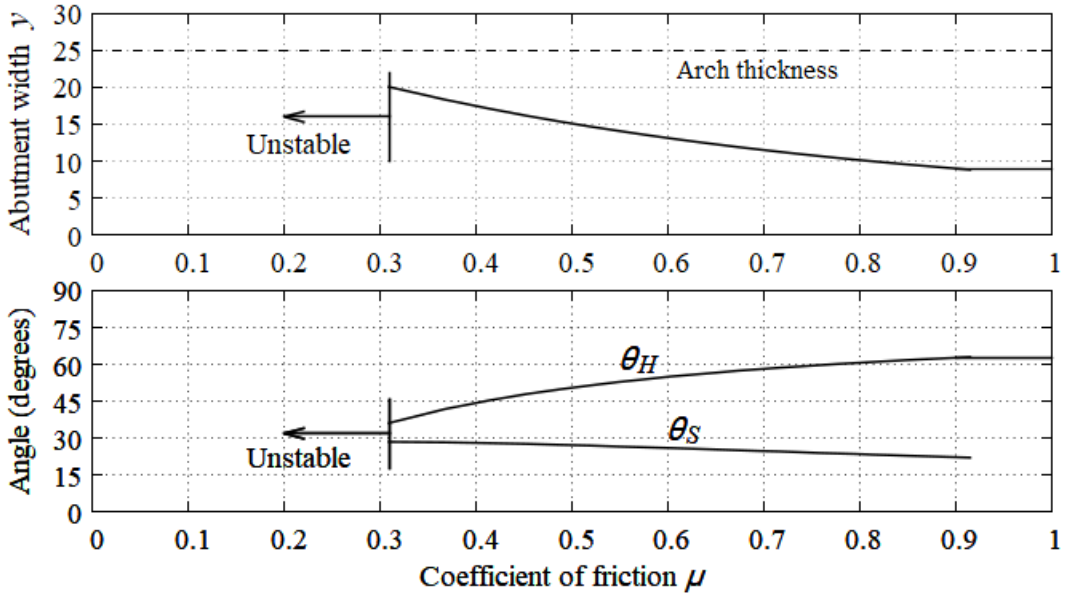

Figure 9: Collapse mechanism parameters for de la Hire's circular arch (actual geometry) over a range of the friction coefficient μ from 0 to 1: abutment width y, hinging joint position angle θ_H and sliding plane position angle θ_S. This plot is for the continuum model.

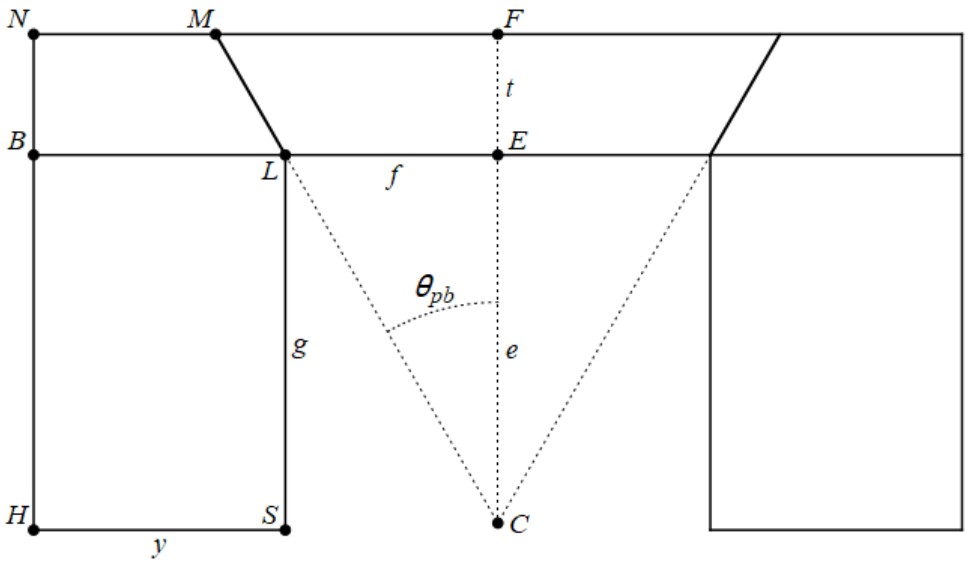

Figure 10. De la Hire's plate-bande. Dimensions in arbitrary units as scaled from Figure A3 are f = 51 (half span), t = 29 (thickness) and g = 90 (height of abutment). θ_{pb} = 30º.

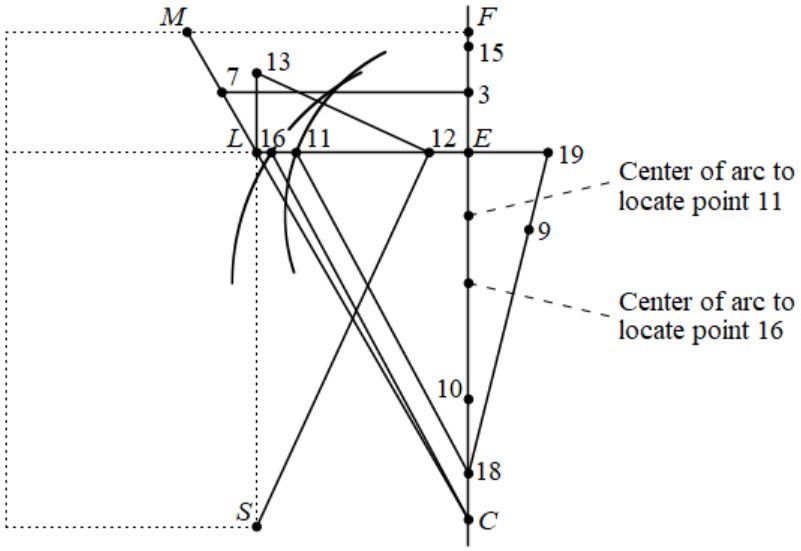

Figure 11. Version of Figure A3 showing the graphical construction to determine abutment width for de la Hire's plate-bande. Length of line 18 9 is the desired abutment width.

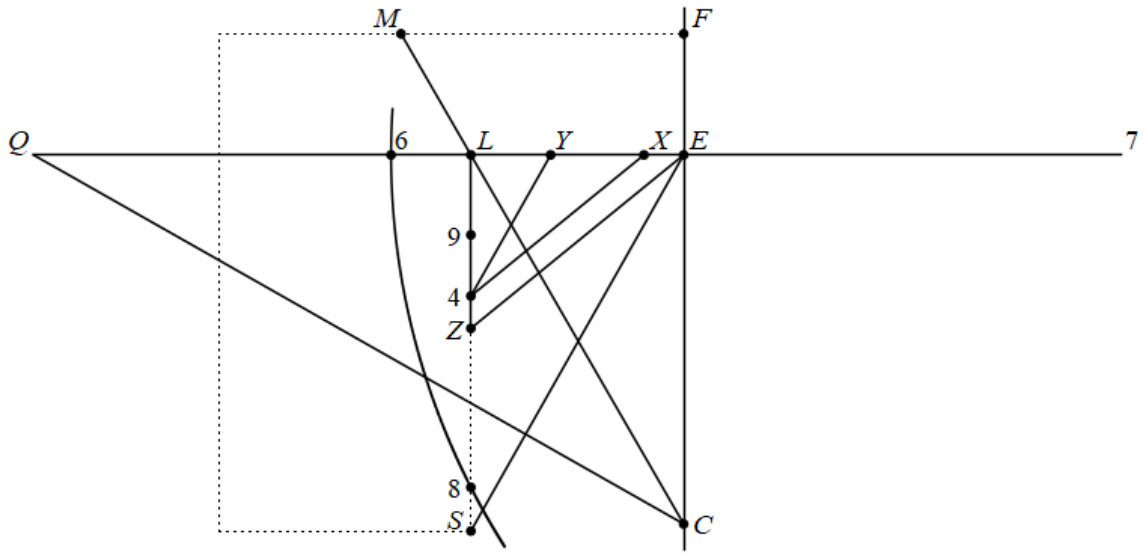

Figure 12. De la Hire's graphical construction method for the circular arch (corrected) applied to the plate-bande. Length of line 98 is the desired abutment width.

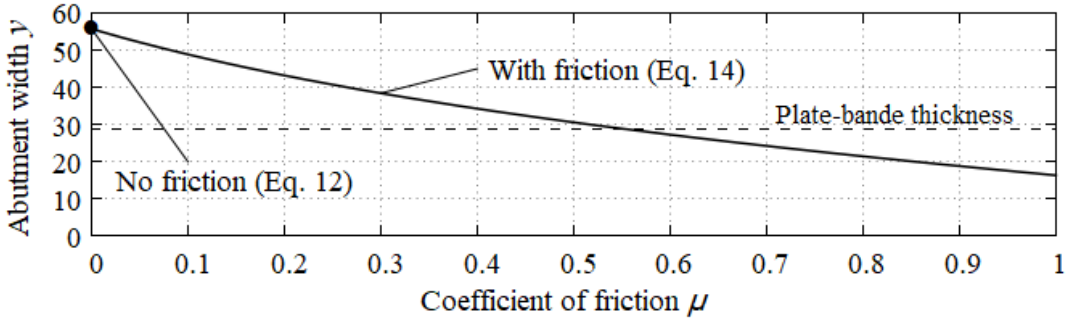

Figure 13. Abutment width predicted by Equation 14 for de la Hire's plate-bande (actual geometry) over a range of the friction coefficient μ from 0 to 1. De la Hire's no-friction solution from Equation 12 is marked. This plot is for the three-piece model.

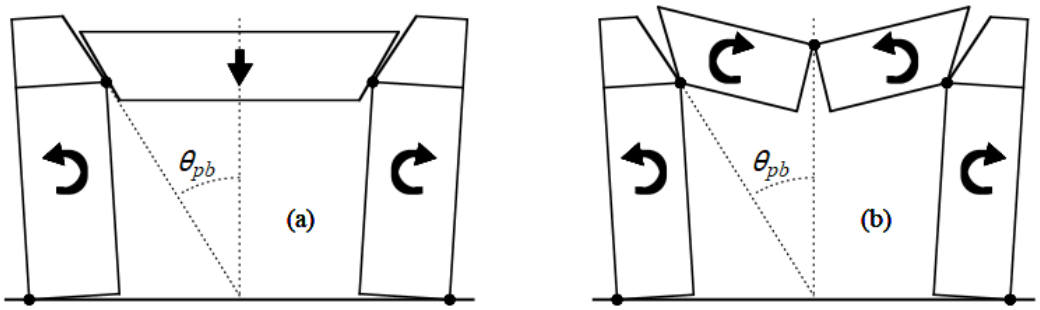

Figure 14. The two collapse mechanisms that occur in a continuum model of de la Hire's plate-bande, depending on the value of the coefficient of friction μ. Sliding along the horizontal joints between the plate-bande and tops of abutments is restrained. Dots denote hinge points. Part (a): Four hinge points with concurrent hinging and sliding along the two inclined joints adjacent to the abutment. Part (b): Hinging only; no sliding.

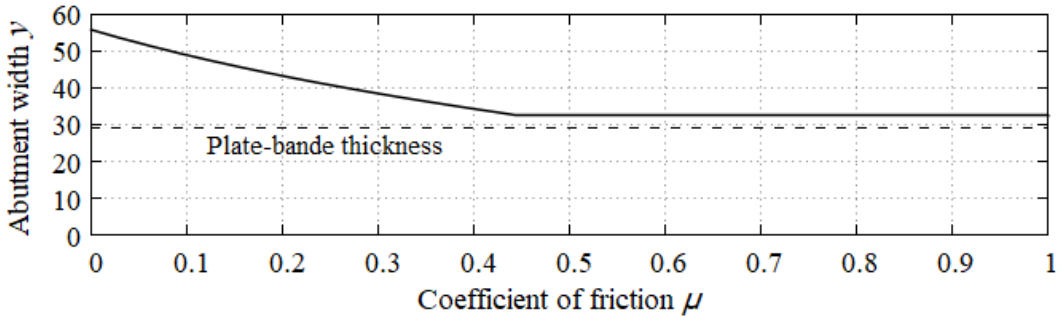

Figure 15. Abutment width y for de la Hire's plate-bande (actual geometry) over a range of the friction coefficient μ from 0 to 1. This plot is for the continuum model.

11. APPENDIX: The three figures from de la Hire's Memoir [2]

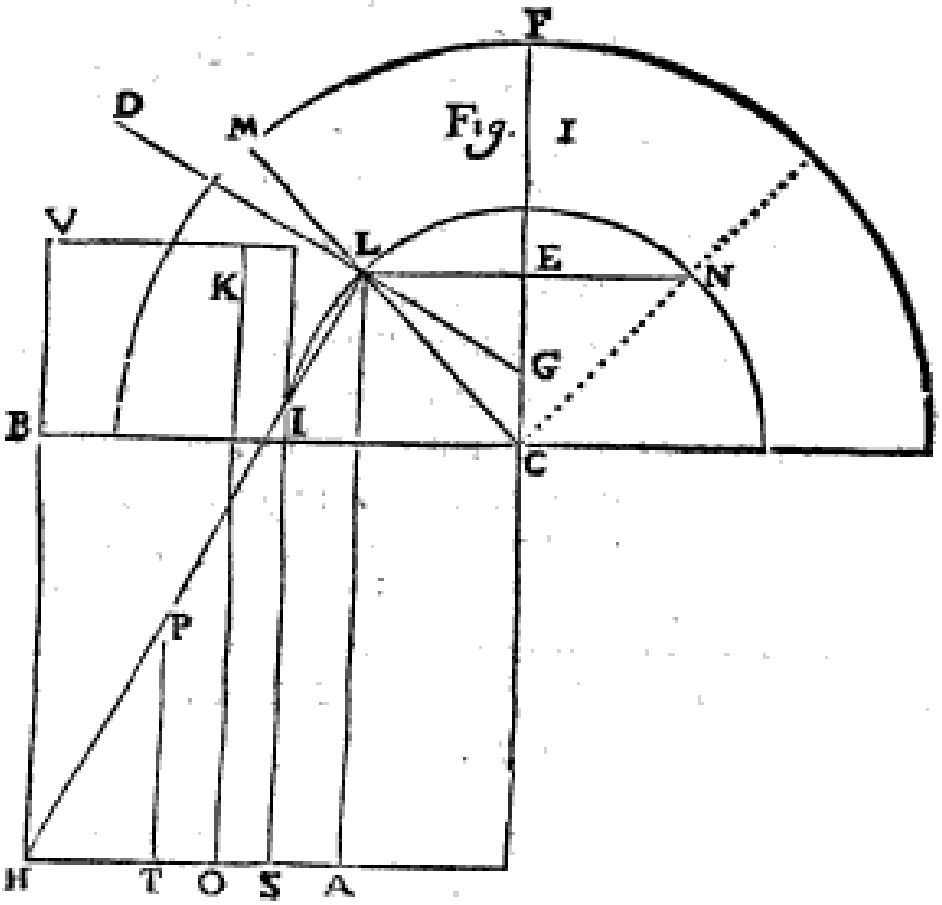

Figure A1. Figure 1 showing circular arch and one abutment together with lines and labels used to derive the equation for abutment width.

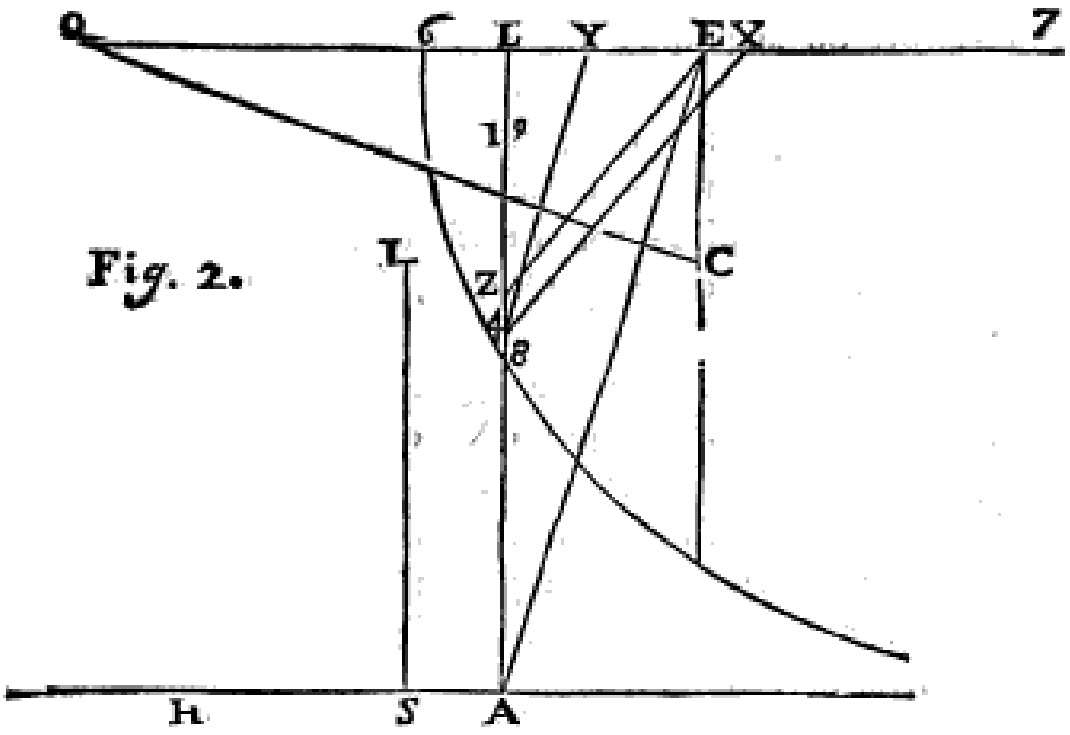

Figure A2. Figure 2 showing the graphical construction used to determine abutment width for the circular arch.

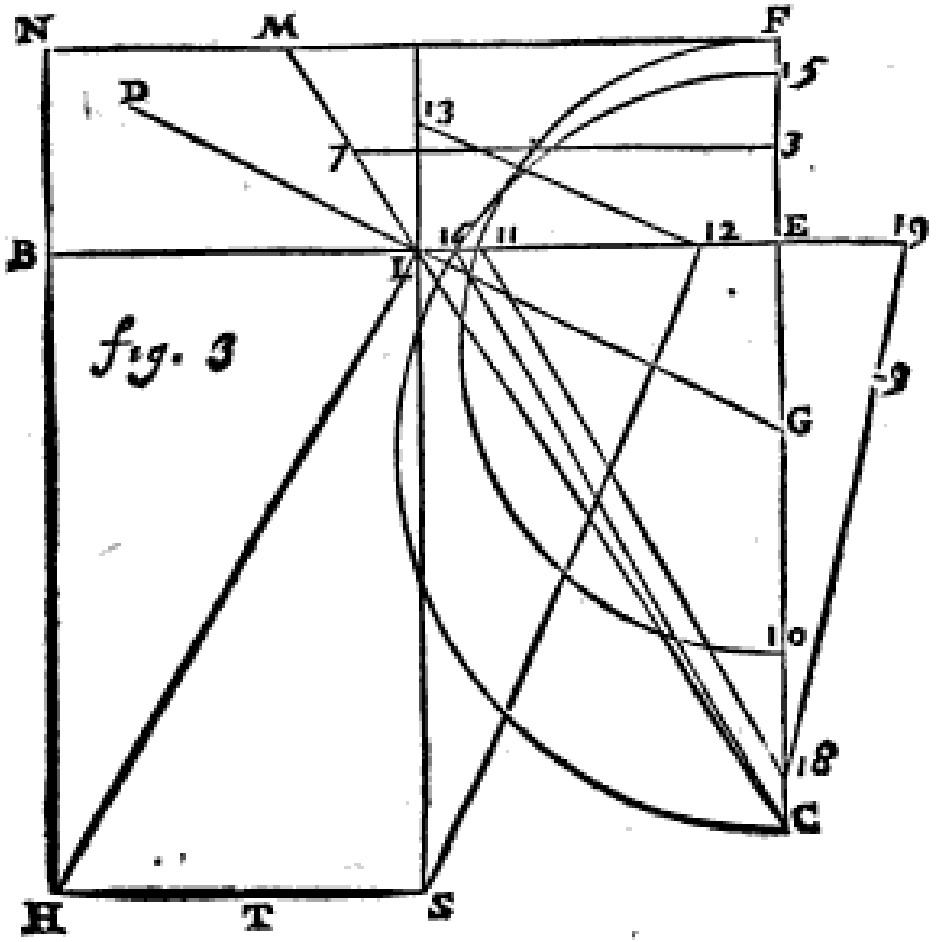

Figure A3. Figure 3 showing the plate-bande to the left of its centerline and the graphical construction used to determine abutment width.